Protein Science (1999), *8*:1878–1887. Cambridge University Press. Printed in the USA.

A comparative study of the unfolding of the endoglucanase Cel45 from *Humicola insolens* in denaturant and surfactant

DANIEL E. OTZEN,[1] LARS CHRISTIANSEN, AND MARTIN SCHÜLEIN

Enzyme Research, Novo Nordisk A/S, DK-2800 Bagsvaerd, Denmark

(RECEIVED February 3, 1999; ACCEPTED May 27, 1999)

Abstract

Cellulases are increasingly being used for industrial purposes, particularly in washing powders, yet little is known of the factors governing the stability of proteins in detergent solutions. We present a comparative analysis of the behavior of the cellulase Cel45 from *Humicola insolens* in the presence of the denaturant guanidinium chloride and the anionic detergent C12-LAS. Although Cel45 unfolds in GdmCl according to a simple two-state model under equilibrium conditions, it accumulates a transient intermediate during refolding. The four disulfide bonds do not contribute detectably to the stability of the native state. Cel45 is unfolded by very low concentrations of C12-LAS (1–4 mM). An analysis of 16 mutants of Cel45 shows a very weak correlation between unfolding rates in denaturant and detergent; mutants that have the same unfolding rate in GdmCl (within a factor of 1.5) vary 1,000-fold in their unfolding rates in C12-LAS. The data support a simple model for unfolding by detergent, in which the introduction of positive charges or removal of negative charges greatly increases detergent sensitivity, while interactions with the hydrophobic detergent tail contribute to a smaller extent. This implies that different detergent-mediated unfolding pathways exist, whose accessibilities depend on individual residues. Double-mutant cycles reveal that mutations in two proximal residues lead to repulsion and a destabilization greater than the sum of the individual mutations as measured by GdmCl denaturation, but they also reduce the affinity for LAS and therefore actually stabilize the protein relative to wild-type. Ligands that interact strongly with the denatured state may therefore alter the unfolding process.

Keywords: alkyl benzene sulfonate; denaturant; detergent; intermediate; protein engineering; protein folding; transition state

Within the last decade, cellulases have achieved significant industrial importance. They have proven commercially useful for "whittling" processes such as modifying pulp fiber surface properties (Jeffries et al., 1992), reducing fuzz, and piling of fabrics and substituting for pumice in stone-washing (Lange, 1993). They have also attracted interest in the detergent industry, due to their ability to brighten faded colored garments by removing loose fluff that would otherwise reflect the light diffusely and give rise to a dull appearance. However, it is not an easy task to obtain a cellulase that functions efficiently under detergent conditions. Insight into the interactions between proteins and detergents is essential. Detergent matrices typically contain both nonionic and ionic detergents (Jakobi & Löhr, 1987). Nonionic or zwitterionic detergents generally stabilize proteins and are often used to solubilize proteins that require a hydrophobic environment, such as membrane proteins (Makino et al., 1973; Clarke, 1975; Casey & Reithmeier, 1993; Renthal & Haas, 1996). In contrast, ionic detergents, particularly anionic detergents, invariably denature proteins partially or completely (Ikai, 1976; Moriyama & Makino, 1985), as exploited in SDS-polyacrylamide gel electrophoresis. However, some proteins have specific detergent binding sites in the native state. For example, serum albumin has 10–11 such sites for single detergent anions, so the protein is actually stabilized against urea denaturation by very low concentrations of anionic detergent (Decker & Foster, 1966).

One of the more prevalent anionic detergents in industrial use is the family of linear alkyl benzene sulfonates (LAS), which typically have 10–18 methylene groups in the alkyl chain. They are biodegradable under aerobic conditions and have higher thermal and chemical stability than other detergents such as soaps and sulfates. However, there is little detailed knowledge of how they denature proteins. Chemical denaturants unfold proteins at molar concentrations because they preferentially stabilize more solvent-

Reprint requests to: Dr. Martin Schülein, Enzyme Research, Novo Nordisk A/S, DK–2800 Bagsvaerd, Denmark; e-mail: mas@novo.dk.

[1]Present address: Department of Biochemistry, University of Lund, P.O. Box 124, S-22100 Lund, Sweden

Abbreviations: CBD, cellulose binding domain; CD, circular dichroism; GdmCl, guanidinium chloride; LAS, linear alkyl benzene sulfonate; UV, ultraviolet.

exposed states (Timasheff, 1993; Baldwin, 1996), though the appropriate interaction model remains a subject of debate (Makhatadze & Privalov, 1992); it is unclear whether the denaturing effect mainly occurs by salting in the peptide backbone (Baldwin, 1996) or by solvating hydrophobic moieties (Tanford, 1970), the latter perhaps through changes in water's structural properties (Vanzi et al., 1998). Detergents inactivate proteins at much lower concentrations, down to 10 μM in the case of C12-LAS (Decker & Foster, 1966). Therefore, their mode of action must involve strong interactions between the detergent molecule and the protein molecule, with preferential binding to the denatured state.

Here, we present a comparative analysis of the behavior of the cellulase Cel45 (formerly known as endoglucanase V) from *Humicola insolens* in the presence of the denaturant guanidinium chloride (GdmCl) and the detergent C12-LAS ($CH_3(CH_2)_{11}$-Ph-SO_3^-). Cel45, which is used in different detergent formulations in the washing industry, belongs to family 45 according to the glucosyl hydrolase classification scheme (Henrissat & Bairoch, 1993), and is a 284-residue protein consisting of a 213-residue catalytic core joined to a 33-residue cellulose binding domain (CBD) via a flexible 38-residue glycosylated linker. This domain arrangement is typical of fungal cellulases (Tomme et al., 1995). The crystal structure of the catalytic core (Davies et al., 1993) reveals a six-stranded β-barrel surrounded by three α-helices and a seventh strand that hydrogen-bonds to the barrel (Fig. 1). Cel45 contains seven disulfide bonds (residue pairs 12–47, 11–135, 89–199, 31–56, 16–86, 87–199, and 156–167) and no *cis* Pro residues. The catalytic domain contains six Trp residues, whose combined fluorescence change on unfolding we use as a probe for following the unfolding process. The structure of the CBD has been solved by NMR (S. Ludvigsen & N. Nordisk, unpubl. obs.) and is identical to the homologous CBD from *Trichoderma reesei* cellobiohydrolase. This is a wedge-shaped β-sheet structure consisting of three antiparallel strands with one hydrophobic and one hydrophilic face (Kraulis et al., 1989).

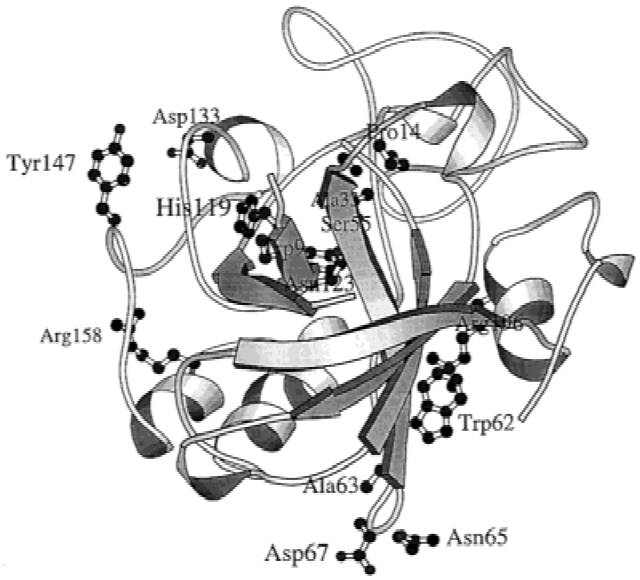

Fig. 1. MOLSCRIPT structure of Cel45 indicating side chains mutated in this study. Drawn using MOLSCRIPT (Kraulis, 1991).

We start our analysis by characterizing the behavior of Cel45 under equilibrium and kinetic conditions in denaturant, showing that at least one transient refolding intermediate is involved in its folding pathway. We then map out the unfolding pathway using 16 Cel45 mutants. This is finally compared with the unfolding behavior of wild-type and the 16 mutants in C12-LAS and the substantial differences are discussed. To our knowledge, this is the first protein engineering study of the effect of detergents on protein unfolding.

Results

The aim of the present study is to characterize Cel45's denaturation process and compare it with the unfolding process induced by the surfactant C12-LAS. We start with a description of the behavior of Cel45 in the presence of the chemical denaturant GdmCl, beginning with wild-type Cel45. Although Cel45 is a multidomain protein, the presence of the linker and the CBD, for which no structure is presently available, does not appear to affect stability and kinetics of folding and unfolding. A truncated version of Cel45 wild-type containing only the catalytic domain showed the same thermodynamic and kinetic properties as the intact enzyme (data not shown). The clear spatial separation between the catalytic domain and the CBD undoubtedly ensures that they fold and unfold independently. Unfolding of CBD does not appears to involve any fluorescence changes, probably because all the Trp residues in the CBD lie on the surface where they bind to cellulose (Kraulis et al., 1989). All mutations discussed in this paper only involve side chains in the catalytic domain. Therefore, the following results only refer to the catalytic domain.

Cel45 unfolds and refolds reversibly according to a two-state model under equilibrium conditions

The equilibrium denaturation of Cel45 in GdmCl (Fig. 2A) represents a single structural transition, in which only the native and denatured states are populated. Secondary and tertiary elements of structure unfold at the same stage, since the far-UV CD and fluorescence denaturation profiles coincide. The same profiles are obtained when starting from unfolded and refolded Cel45, implying that chemical denaturation is completely reversible. In contrast, thermal denaturation at pH 7.0 in the absence of denaturant is completely irreversible, even when the temperature rise is reversed at a stage where the unfolding has just reached completion (87 °C, D.E. Otzen & M. Schülein, unpubl. data). The equilibrium data for unfolding in GdmCl fit the two-state model (Table 1).

Although Cel45 contains seven disulfide bridges, two of which link side chains more than 100 residues apart, the reduced form is not less stable than the oxidized form. The midpoint of denaturation is slightly lower (2.60 M vs. 3.05 M in the absence of DTT), but this is compensated by the small increase in the value of $m_{N\text{-}U}$ (4.56 M^{-1} vs. 3.54 M^{-1} in the absence of DTT). The reduction of disulfide bonds is expected to increase the value of $m_{N\text{-}U}$ (which is a rough measure of the difference in solvent exposure between the native and denatured states), since the removal of covalent cross-links raises the denatured state's level of conformational freedom and solvent exposure (Pace et al., 1988). However, the small decrease in $m_{N\text{-}U}$ indicates that the disulfide bonds do not make the denatured state significantly more compact and therefore do not stabilize them very much. Previous work suggests that a covalent

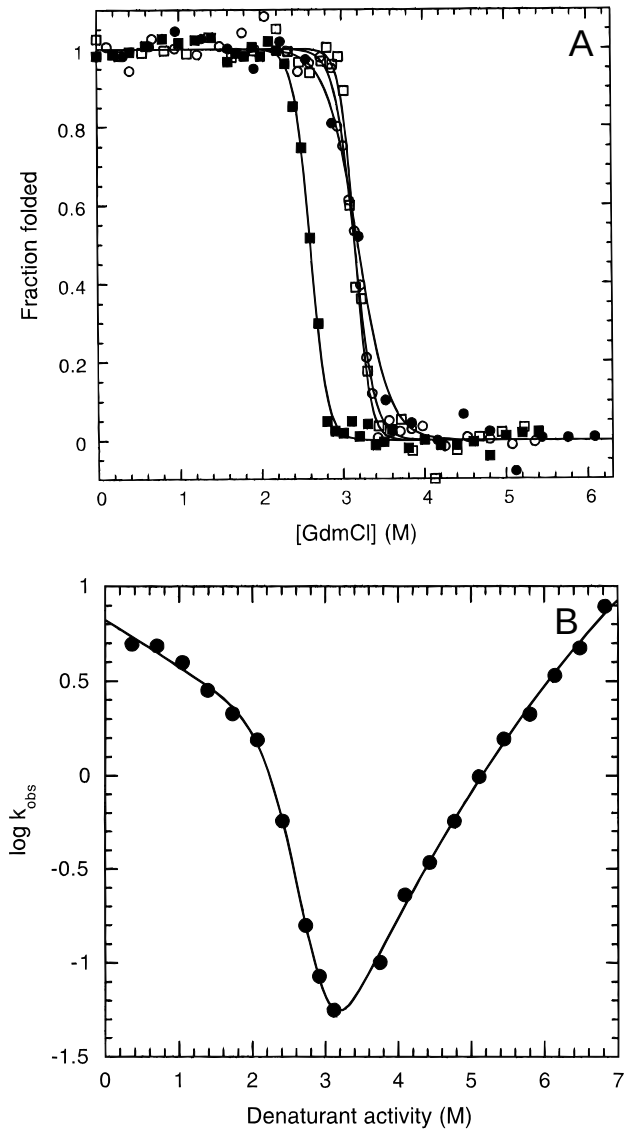

Fig. 2. A: Equilibrium denaturation of Cel45 wild-type measured by peptide CD (ellipticity at 220 nm, filled circles) and fluorescence. Fluorescence data were obtained by diluting a concentrated stock of either native (empty squares) or denatured (empty circles) Cel45 into aliquots of increasing GdmCl concentration. Denaturation of Cel45 in 10 mM DTT (filled squares) also shown. **B:** Chevron plot for Cel45 wild-type. Rate constants in s^{-1}. Data were fitted to Equation 8.

Table 1. *Summary of thermodynamic parameters for Cel45 wild-type*[a]

Parameter	Value
$D^{50\%}$(equilibrium) (M)[b]	3.05 ± 0.01
$m_{N\text{-}U}$ (equilibrium) (M^{-1})[b]	3.54 ± 0.25
$D^{50\%}$(kinetic) (M)[c]	3.02 ± 0.11
$m_{N\text{-}U}$ (kinetic) (M^{-1})[d]	2.94 ± 0.14
$D^{50\%}_{red}$ (equilibrium) (M)[e]	2.60 ± 0.01
$m^{red}_{N\text{-}U}$ (equilibrium) (M^{-1})[e]	4.56 ± 0.27
$\Delta G^{water}_{U\text{-}F}$ (equilibrium) (kcal mol^{-1})[f]	14.7 ± 0.76
$\Delta G^{water}_{U\text{-}F}$ (kinetic) (kcal mol^{-1})[g]	13.5 ± 1.47
$\Delta G^{water,red}_{U\text{-}F}$ (equilibrium) (kcal mol^{-1})[e]	16.1 ± 0.63
k_f^{water} (s^{-1})[h]	6.66 ± 0.33
m_f (M^{-1})[h]	−0.25 ± 0.04
K_I^{water}[h]	(39.8 ± 3.9) × 10^3
m_I (M^{-1})[h]	−2.03 ± 0.15
k_u^{water} (s^{-1})[h]	(3.15 ± 0.24) × 10^{-5}
m_u (M^{-1})[h]	1.15 ± 0.13
m_u^* (M^{-2})[h]	−0.053 ± 0.013
β^I[i]	0.64
$\beta^{\ddagger}$[j]	0.82

[a] All experiments in the absence of reducing agent except where indicated.
[b] Calculated using the two-state model for equilibrium unfolding (Equation 5).
[c] Calculated as the denaturant concentration where the refolding and unfolding limbs intercept, i.e., where $\log k_u = \log(k_f/(1 + 1/K_I))$.
[d] $m_{N\text{-}U}$(kinetic) = $m_f + m_I + m_u$.
[e] Under reducing conditions (10 mM DTT).
[f] $\Delta G^{water}_{U\text{-}F}$ (equilibrium) = 1.36 ∗ $m_{N\text{-}U}$ ∗ $D^{50\%}$.
[g] $\Delta G^{water}_{U\text{-}F}$ (kinetic) = 1.36 ∗ ($\log K_I^{water} + \log(k_f^{water}/k_u^{water})$).
[h] Calculated using Equation 7.
[i] The position of the refolding intermediate on the reaction coordinate (Equation 2).
[j] The position of the transition state between the intermediate and the native state on the reaction coordinate (Equation 3) at the midpoint of denaturation.

cross-link's entropic contribution to protein stability may be estimated from the equation:

$$\Delta S_{conf} = -2.1 - 3/2R \ln n \quad (1)$$

where n is the number of residues between the cross-linked side chains (Pace et al., 1988). Thus, the disulfide bond between Cys11 and Cys135 should stabilize Cel45 by 4.9 kcal/mol alone. Perhaps the absence of cross-links allows other hydrophobic clusters to form. In contrast, removal of both disulfide bonds in RNase T_1 (between residues 2–10 and 6–103) increased $m_{U\text{-}F}$ by ca. 50% (Pace et al., 1988), while the introduction of a disulfide bond into the 64-residue chymotrypsin inhibitor 2, linking residues 2 and 63, decreased $m_{U\text{-}F}$ to 60% of the original value (Otzen & Fersht, 1998). Reduction of the single disulfide bond in endoglucanase EGIII from *T. reesei* (only spanning 29 residues) reduces stability by 7 kcal mol (Arunachalam & Kellis, 1996), although Equation 19 would predict only 3.6 kcal/mol.

The kinetics of folding of Cel45 are not two-state

Unfolding and refolding of Cel45 show double exponential kinetics, in which the slow and the fast phases are clearly separated. For the purpose of the present analysis, we concentrate on the fast phase and refrain from speculating on the nature of the slow phase. The logarithm of the observed rate constant (k_{obs}) is plotted against denaturant concentration in Figure 2B. The roll over (reduction in slope) at low denaturant concentration is indicative of the accumulation of a transient refolding intermediate under native-like refolding conditions. Log k_u manifests a slightly parabolic dependence on denaturant concentration, similar to barnase (Matouschek & Fersht, 1993); this is not necessarily indicative of an unfolding intermediate, but may be due to solvent effects (Parker

et al., 1995). The joined line is the best fit to Equation 7, which includes a folding intermediate, and the fitted parameters (Table 1) reveal a satisfactory correspondence between equilibrium and denaturation data. To date, the largest protein to fold and unfold without intermediates is the 126-residue vilin 14T (Choe et al., 1998). Therefore, it is not surprising that the 213-residue catalytic core of Cel45 accumulates at least one intermediate during its refolding process. The intermediate is 8.8 kcal mol^{-1} more stable than the unfolded state in the absence of denaturant, but due to its compactness it is very sensitive to denaturant, and the two states are equally stable (and thus equally populated) at 1.74 M GdmCl; at the midpoint of denaturation, the intermediate is 2.4 kcal mol^{-1} less stable. Thus, the rate limiting step changes from the conversion of *I* to the transition state (below 1.74 M) to the conversion of *U* to *I* (above 1.74 M).

The folding process may be viewed as a reaction going from the unfolded state (reaction coordinate $\beta^U = 0$) to the native state (reaction coordinate $\beta^N = 1$) (Tanford, 1970). The positions of the intermediate (β^I) and transition state ($\beta^{\ddagger}$) on the folding reaction coordinate may be calculated from the following relationships (Tanford, 1970):

$$\beta^I = m_I/(m_f + m_I + m_u) \quad (2)$$

$$\beta^{\ddagger} = (m_I + m_f)/(m_f + m_I + m_u). \quad (3)$$

These values approximate the extent to which the surfaces of the intermediate and the transition state have become excluded from denaturant (and thus to solvent), expressed as the fraction of the surface area buried compared to the native state. The fact that $\beta^I = 0.65$ and $\beta^{\ddagger} = 0.78$ reveals that most of the surface area, accessible in the unfolded state but buried in the native state, is already buried in the intermediate, and only becomes slightly less solvent-exposed in the major transition state. By comparison, the 175-residue N-terminal fragment of phosphoglycerate kinase has a β^I-value of 0.70 and a $\beta^{\ddagger}$-value of 0.80 (Parker et al., 1995).

Characterization of the unfolding step by protein engineering

Cel45's unfolding step involves the major transition state between the native and the intermediate. We have characterized this state by protein engineering using Φ-value analysis (Matouschek et al., 1989; Fersht et al., 1992). In this approach, a suitable side chain is truncated by site-directed mutagenesis and the effect of the mutation on the protein's thermodynamic stability ($\Delta\Delta G_{N\text{-}U}$) and activation energy of unfolding ($\Delta\Delta G_{N\text{-}\ddagger}$) is measured. If the side chain is in a native-like environment in the transition state, both the native state and the transition state will be destabilized to a similar extent by the mutation, which means that $\Delta\Delta G_{N\text{-}\ddagger} = 0$ (i.e., the mutant unfolds at the same rate as the wild-type) and the parameter $\Phi_u = \Delta\Delta G_{N\text{-}\ddagger}/\Delta\Delta G_{N\text{-}U} = 0$. Conversely, if the side chain is in a denatured environment in the transition state, $\Delta\Delta G_{N\text{-}\ddagger} = \Delta\Delta G_{N\text{-}U}$ and $\Phi_u = 1$.

Fourteen single mutations, one double mutation, and one triple mutation have been analyzed (Table 2; Fig. 1). Despite being surface-exposed, the mutations destabilize Cel45 by up to 5 kcal mol^{-1} under equilibrium conditions (Table 3). The two most destabilizing mutants (the double and the triple mutant) introduce two or three positive mutations in close proximity, leading to charge repulsion and weakening of the native structure. In contrast, two mutations (S55M and N123A) actually stabilize Cel45 by ca. 1 kcal mol^{-1}.

Table 2. *Cel45 mutants studied in this paper*

Mutation	Position in Cel45	Original rationale for design
W9F	Loop 1 just after β-strand 1	Enzyme activity
P14A	Loop 1	Enzyme activity
A33P	Loop 1	Stability
S55M	Loop 1	Stability
W62E	β-strand 2	Surfactant sensitivity
A63R	β-strand 2	Surfactant sensitivity
N65R	Loop after β-strand 2	Surfactant sensitivity
D67R	Loop after β-strand 2	Surfactant sensitivity
N65R/D67R	Loop after β-strand 2	Surfactant sensitivity
A63R/N65R/D67R	β-strand 2 and loop	Surfactant sensitivity
H119Q	Edge of β-barrel (β-strand 6)	Activity
N123A	β-strand 6	Activity
D133N	Loop near active site	Surfactant sensitivity
Y147G	Loop near active site	Activity
R158E	α-helix 1	Surfactant sensitivity
R196E	α-helix 3	Surfactant sensitivity

Hammond-type behavior of Cel45

At 5 M GdmCl, there is a 600-fold variation in k_u for the 16 Cel45 mutants; the difference becomes even more pronounced at lower denaturant concentrations because of the large variations in m_u between different mutants (Table 4). m_u also varies with concentration because of unfolding curvature, but when m_u is calculated

Table 3. *Equilibrium parameters for Cel45 mutants*

Mutant	$[D]^{50\%}$ (M)[a]	$m_{N\text{-}U}$ (M^{-1})	$\Delta\Delta G_{N\text{-}U}$ (kcal mol^{-1})[b]
Wild-type	3.05 ± 0.01	3.54 ± 0.25	0
W9F	2.46 ± 0.02	5.93 ± 0.60	3.96 ± 0.31
P14A	2.65 ± 0.02	3.48 ± 0.37	2.69 ± 0.21
A33P	2.67 ± 0.02	6.29 ± 1.04	2.55 ± 0.20
S55M	3.38 ± 0.02	6.70 ± 0.93	−2.22 ± 0.17
W62E	2.40 ± 0.01	6.20 ± 0.35	4.37 ± 0.34
A63R	2.78 ± 0.02	5.05 ± 0.37	1.81 ± 0.14
N65R	2.58 ± 0.01	6.09 ± 0.31	3.16 ± 0.24
D67R	2.99 ± 0.02	3.56 ± 0.39	0.40 ± 0.03
N65R/D67R	2.34 ± 0.02	3.89 ± 0.32	4.77 ± 0.37
A63R/N65R/D67R	2.20 ± 0.02	5.36 ± 0.87	5.71 ± 0.45
H119Q	3.01 ± 0.02	3.87 ± 0.41	0.27 ± 0.02
N123A	3.36 ± 0.01	5.84 ± 0.42	−2.08 ± 0.16
D133N	2.70 ± 0.02	4.03 ± 0.60	2.35 ± 0.18
Y147G	2.82 ± 0.02	4.18 ± 0.31	1.55 ± 0.12
R158E	3.13 ± 0.01	4.80 ± 0.32	−0.54 ± 0.04
R196E	2.61 ± 0.01	5.15 ± 0.31	2.96 ± 0.23

[a] Denaturant concentration.
[b] Calculated using Equation 6.

Table 4. *Parameters for unfolding of Cel45 mutants in GdmCl and C12-LAS*

Mutant	$k_u^{1.23\,mM}$ (min^{-1})[a]	Activity in LAS pH 7[b]	$k_u^{5\,M}$ (s^{-1})[c]	$m_u^{5\,M}$ (M^{-1})[d]	$\Delta\Delta G_{N\text{-}\ddagger}^{5\,M}$ (kcal mol^{-1})[e]	$1 - \Phi_u^{5\,M}$[f]
Wild-type	0.48	100	0.81 ± 0.16	0.62 ± 0.02	0	0
W9F	0.034	—	57.3 ± 0.57	0.29 ± 0.02	2.52 ± 0.06	0.36 ± 0.03
P14A	1.43	—	2.73 ± 0.12	0.46 ± 0.04	0.72 ± 0.02	0.73 ± 0.06
A33P	0.48	32	2.95 ± 0.06	0.70 ± 0.02	0.77 ± 0.02	0.70 ± 0.06
S55M	0.17	96	0.17 ± 0.01	0.86 ± 0.08	−0.92 ± 0.04	0.59 ± 0.05
W62E	0.80	50	1.85 ± 0.16	0.54 ± 0.05	0.49 ± 0.02	0.89 ± 0.08
A63R	2.21	36	0.68 ± 0.15	0.84 ± 0.16	−0.10 ± 0.01	1.1 ± 0.13
N65R	1.08	46	2.15 ± 0.17	0.58 ± 0.09	0.58 ± 0.03	0.82 ± 0.07
D67R	3.65	39	0.94 ± 0.18	0.54 ± 0.02	0.09 ± 0.01	0.78 ± 0.07
N65R/D67R	0.096	39	1.25 ± 0.13	0.71 ± 0.01	0.26 ± 0.01	0.95 ± 0.08
A63R/N65R/D67R	0.08	211	0.91 ± 0.07	0.65 ± 0.02	0.07 ± 0.01	0.99 ± 0.09
H119Q	0.17	146	1.79 ± 0.13	0.68 ± 0.01	0.47 ± 0.01	0.30 ± 0.01
N123A	0.15	214	0.09 ± 0.01	1.1 ± 0.08	−1.28 ± 0.08	0.38 ± 0.04
D133N	152	0	9.37 ± 0.57	0.66 ± 0.14	1.45 ± 0.08	0.38 ± 0.04
Y147G	9.8	—	4.70 ± 0.17	0.74 ± 0.02	1.04 ± 0.03	0.33 ± 0.03
R158E	0.005	325	0.69 ± 0.12	0.69 ± 0.02	−0.09 ± 0.01	—[g]
R196E	0.075	75	1.74 ± 0.28	0.52 ± 0.03	0.45 ± 0.02	0.85 ± 0.08

[a] Rate of unfolding in 1.23 mM C12-LAS.
[b] Data from B. Damgaard based on assay for releasing reducing ends from Avicel (unpubl. data).
[c] Rate of unfolding in 5 M GdmCl; unfolding data fitted to Equation 8.
[d] Calculated using Equation 9.
[e] Calculated using Equation 10.
[f] $\Phi_u^{3\,M} = \Delta\Delta G_{N\text{-}\ddagger}^{3\,M}/\Delta\Delta G_{N\text{-}U}$.
[g] Not applicable because $\Delta\Delta G_{N\text{-}U}$ is very close to zero.

at a fixed denaturant concentration (5 M), we observe a reasonable linear relationship between m_u and the destabilization energy of unfolding, $\Delta\Delta G_{N\text{-}\ddagger}^{5M}$ ($R = 0.86$, Fig. 3B). The positive slope in this plot (which is 0.07 ± 0.02 when normalized relative to $m_{N\text{-}U}$) means that as $\Delta\Delta G_{N\text{-}\ddagger}$ becomes more negative (the transition state becomes more destabilized), m_u becomes smaller. Since *m*-values are interpreted as measures of the difference in solvent-exposure between the two states involved in a given reaction (Tanford, 1970), the decrease in the value of m_u means that the transition state and the native state move closer to each other. This is a clear example of the behavior predicted in the Hammond postulate (Hammond, 1955), which states that two neighboring states in a reaction move closer to each other along the reaction coordinate as the energy difference between them decreases. Hammond-type behavior has been observed for smaller proteins, namely the 110-residue barnase (Matouschek & Fersht, 1993) and the 64-residue CI2 (Matouschek et al., 1995). The sensitivity of the structure of Cel45's transition state to destabilization (0.07 mol $kcal^{-1}$) is comparable to that of barnase and CI2 (Matouschek & Fersht, 1993; Matouschek et al., 1995) (0.037 ± 0.005 and 0.06 ± 0.01 mol $kcal^{-1}$, respectively).

Φ_u-value analysis of the unfolding of Cel45

The results of the Φ_u-value analysis are shown in Table 4. To make the data more transparent, the final column lists $1 - \Phi_u$ rather than Φ_u; thus, the higher the value of $1 - \Phi_u$ is for a given mutation, the more native-like is the structure in the transition state around the mutated side chain. In Φ-analysis, the mutation in question should ideally remove side-chain interactions (as in P14A or D133N) rather than substitute them with others (as in W62E or A63R). Note, however, that the mutant A63R can be visualized as the pseudo wild-type for the simple mutation Arg63 → Ala, whose $(1 - \Phi_u)$-value of 1.08 is readily interpretable. All the different mutations in the area around β-strand 2 (residues 62–67 and α-helix 3) have $(1 - \Phi_u)$-values around 1, which suggests that this region remains native-like in the transition state. The residues in loops (S55 and Y147), at the end of β-strand 6 (N123), in α-helix 1 (R158), and the active site (including His119 and Trp9) have fractional $(1 - \Phi_u)$-values, which are more difficult to interpret, although most of the mutations in these regions involve chemically sensible truncations. They may indicate partially formed interactions or parallel unfolding pathways (Fersht et al., 1994).

The principal aim of the present study is not to carry out an exhaustive characterization of the transition state of Cel45 at the same level of detail as barnase (Serrano et al., 1992), but rather to compare the unfolding of Cel45 in GdmCl and surfactant. However, according to the principle of microscopic reversibility, the major transition state of unfolding is also the transition state of refolding. Therefore, it appears from our limited amount of data that Cel45 refolds in distinct domains: parts of the β-sheet structure and the nearby α-helix 3 are completely formed in the transition state, while the loops and α-helix 1 may be partially unfolded and only fold completely at a later stage.

Denaturation of Cel45 in C12-LAS

In 50 mM HEPES pH 7 at 25 °C, C12-LAS′ critical micelle concentration is 0.7 mM; below this concentration, it exists predominantly as monomers, and above this concentration, as micelles. Based on activity measurements, C12-LAS is known to inactivate Cel45 at pH 7 in the 200–1000 ppm range (B. Damgaard, unpubl.

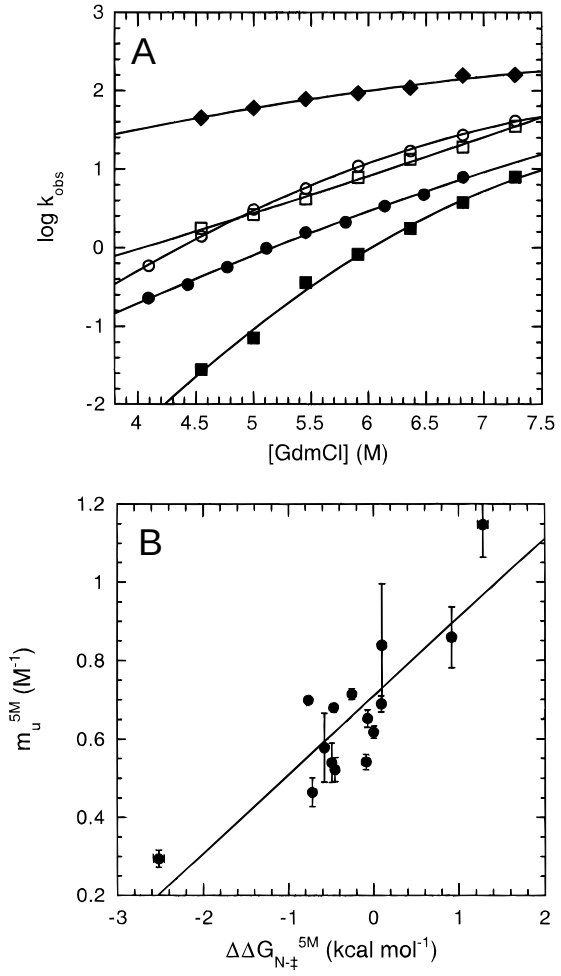

Fig. 3. A: The logarithm of the unfolding rates plotted vs. denaturant concentration for Cel45 wild-type and four mutants, A33P (empty circles), N123A (filled squares), P14A (empty squares), and W9F (filled diamonds). Rate constants in min^{-1}. **B:** Hammond plot of the m_u-values of individual mutants vs. the change in the activation free energy of unfolding ($\Delta\Delta G_{N-\ddagger}$). The linear fit has a slope of 0.20 ± 0.03 (correlation coefficient 0.86). The significant linearity argues for pronounced Hammond behavior in the unfolding of Cel45.

obs.). When Cel45 is incubated with C12-LAS at these concentrations, there is a slow mono-exponential decline in the fluorescence signal and the rate constant associated with this decline increases with surfactant concentration. The length of the alkyl chain correlates with increasing aggressiveness towards the protein; C11-LAS is less potent than C12-LAS, which in turn is eclipsed by C13-LAS (Fig. 4A). Near-UV spectra (not shown) indicate a complete loss of tertiary structure in the presence of C12-LAS; however, due to the high absorption of C12-LAS in the far-UV range, it was not possible to determine whether surfactant-unfolded Cel45 possessed native like secondary structure.

There is not a linear relationship between [C12-LAS] and log k_{unf}; instead, log k_{unf} appears to approach an asymptotic value at high surfactant concentrations. A linear relationship would indicate weak, unspecific binding. In the case of chemical denaturants such as GdmCl and urea, this has been ascribed to weak interactions of denaturant with the peptide backbone and solvation of hydropho-

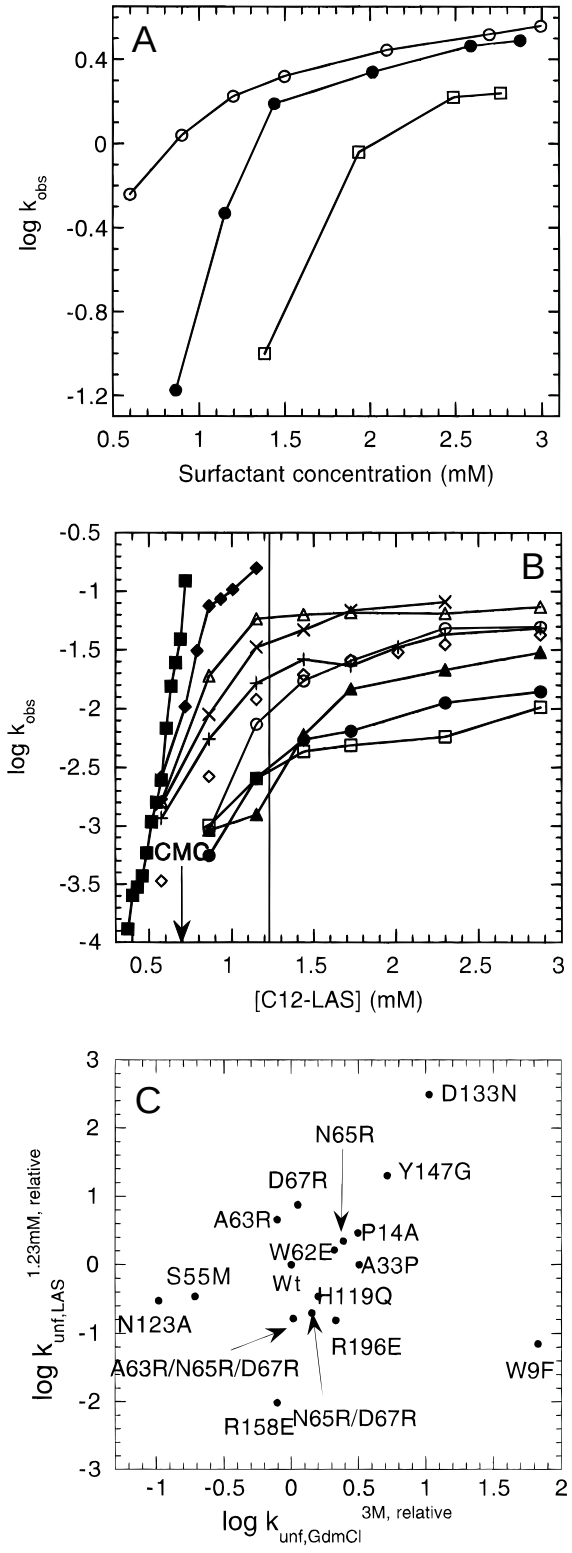

Fig. 4. A: Unfolding of wild-type Cel45 in detergents of different chain lengths, namely C11 (empty circles), C12 (filled circles), and C13 (empty squares). Rate constants in min^{-1}. **B:** Rate of unfolding of several Cel45 mutants vs. [C12-LAS]: wild-type (empty circles), S55M (empty squares), W62E (empty diamonds), A63R (×), N65R (+), D67R (empty triangles), H119Q (filled circles), D133N (filled squares), Y147G (filled diamonds), and R196E (filled triangles). Rate constants in min^{-1}. **C:** Log relative unfolding rates of Cel45 mutants in 5 M GdmCl vs. log relative unfolding rates in 1.23 ppm C12-LAS. Note the absence of a clear linear relationship.

bic moieties, favoring the more highly solvated denatured state (Tanford, 1970). This is the basis for the sequence-independent effect of denaturants on proteins, which make them highly appropriate for measuring proteins' thermodynamic properties. However, surfactants have an effect at concentrations three orders of magnitude below those of GdmCl and urea, indicating an altogether different and more specific mode of action. Lower concentrations of C12-LAS were required to denature Cel45 at lower protein concentrations (data not shown), suggesting either stoichiometric binding or formation of complexes involving several protein molecules, as observed in other detergent systems (Ray et al., 1966). This precludes refolding studies with surfactant, since refolding from a concentrated solution of protein unfolded in surfactant dilutes out both surfactant and protein. Nevertheless, denaturation of Cel45 by surfactant is a reversible process; endoglucanase activity can be recovered after extensive dialysis (M. Schülein, unpubl. obs.).

It is not clear which kinetic model should be used to fit the unfolding. The equation for a simple binding process,

$$N + D_n \underset{k_{-1}}{\overset{k_1}{\rightleftarrows}} N{:}D_n \xrightarrow{k_{unf}} U{:}D_n,$$

in which D_n represents a detergent micelle (whose concentration is 0 below ca. 220 ppm, above which it rises proportionally with the increase in total detergent concentration) fits the kinetic data poorly (data not shown). It is possible that more micelles will bind to the protein as the detergent concentration increases; proteins are known to bind detergent ions in successive stages (Tanford, 1991).

The different Cel45 mutants show the same monotonic increase in unfolding rate with increasing [C12-LAS]. The greatest variation in $\log k_{unf}$ between the mutants is seen around 1.23 mM (400 ppm). We, therefore, use the unfolding rate at 1.23 mM as an indication of the kinetic stability of Cel45 mutants in C12-LAS (Table 4; Fig. 4B). Note the correlation between the unfolding rates of the various mutants in C12-LAS and their enzymatic activity in detergent: all mutants that have higher activity than wild-type unfold significantly more slowly and, therefore, remain active for a longer time during the activity assay, while the opposite applies to mutants with lower activity. This supports the notion that our fluorescence measurements in the presence of C12-LAS are measuring a genuine denaturation process rather than just a build-up of micelles on the surface of the native protein, for example.

When the log of the relative unfolding rate in 400 ppm C12-LAS is plotted vs. its equivalent in 3 M GdmCl (Fig. 4C), the lack of correlation between the two parameters is revealed (a linear fit yields $R = 0.24$). Wild-type Cel45, A63R, N65R, D67R, N65R/D67R,A63R/N65R/D67R, and R158E unfold at nearly the same rate in 3 M GdmCl (varying within a factor 1.5), yet their unfolding rates in C12-LAS vary 1,000-fold. Conversely, S55M unfolds five times faster than W9F in C12-LAS, but unfolds 350 times slower in GdmCl. The two modes of denaturation appear to be different, although there is a weak trend that sensitivity to denaturant accompanies sensitivity to detergent.

Discussion

Like all denaturants, C12-LAS denatures Cel45 because it binds with greater affinity to the denatured state than the native state. Individual detergent molecules can bind tightly and noncooperatively to native bovine serum albumin (Tanford, 1991) and lysozyme (Yonath et al., 1977), usually 1 detergent per cationic residue (Bordbar et al., 1997). This stabilizes the native state. However, up to 76 C12-LAS molecules bind in a cooperative fashion to a single molecule of denatured serum albumin, probably as micelles bound to a few sites (Turro et al., 1995). The susceptibility to unfolding of different Cel45 mutants is dependent on the degree of stabilization of the native state, the facility with which micelles form in the denatured state and how they stabilize transition states and possible intermediates in the unfolding pathway. Note that several mutants denature in C12-LAS at concentrations below the CMC (0.7 mM), in particular D133N, which is denatured at concentrations as low as 0.4 mM. In other words, individual detergent molecules may bind tightly enough to Cel45 to denature the protein. It is also possible, however, that the protein facilitates clustering of detergent molecules at concentrations below the CMC in solution, perhaps by reducing the repulsion between the charged sulfate groups. SDS forms a 3-micellar compex on PRAI at 1.6 mM, although its CMC in solution is 1.8 mM (Ibel et al., 1990).

While a protein in 6 M GdmCl is essentially completely unstructured (Tanford, 1968), no dramatic increase in the hydrodynamic radius accompanies binding of detergent. There appears to be a large degree of ordered, albeit nonnative, structure, and several structural models have been proposed for the protein-detergent complex (Jirgensons, 1967; Reynolds & Tanford, 1970; Mattice et al., 1976; Mascher & Lundahl, 1989; Rao, 1989; Ibel et al., 1990; Tanford, 1991). Since the endpoint of the denaturation process is different, the process itself is also likely to be different. This is borne out by the lack of correlation for Cel45 between unfolding rates in GdmCl and detergent (Fig. 4C). There are probably different unfolding routes available in the presence of detergent; which of them is preferred depends to a large extent on individual residues. Residues 133 and 158, though far apart in the native structure, both act as nucleation centers for unfolding in detergent; the mutations Asp → Asn133 and Arg → Glu158, respectively, increase and reduce unfolding rates by two orders of magnitude. This is much larger than the effect on the unfolding rates in GdmCl.

We interpret the effect of the Cel45 mutations in simple electrostatic-hydrophobic terms, in which the detergent initially binds to the protein through electrostatic attraction to positively charged side chains on the surface; subsequent unfolding facilitates contact between the alkyl chain and the hydrophobic core of the protein (cf. Bordbar et al., 1997; Yonath et al., 1977). In line with this, increasing the length of the alkyl chain from C11-LAS to C13-LAS increases the unfolding rate (Fig. 4A) by increasing the contact area between protein and detergent. Because of the negative charge on the sulfonate group, the introduction of a negative charge or removal of a positive charge is *ceteris paribus* expected to decrease the affinity of C12-LAS for the protein, leading to a greater stability of the protein in the presence of the surfactant. This explains qualitatively why R158E and R196E are stabilized relative to wild-type, while A63R, N65R, D67R, and D133N are destabilized. The remaining seven mutants (except W9F) show a relatively weak correlation ($R = 0.72$) between unfolding rates in GdmCl and C12-LAS. This may reflect an underlying similarity betwen GdmCl and C12-LAS in terms of interactions with hydrophobic side chains. GdmCl is known to solvate hydrophobic side chains (Nozaki & Tanford, 1970; Parker et al., 1995),

and C12-LAS′ hydrophobic tail (the alkyl chain and the benzene group) may exert a similar effect. However, the electrostatic interaction is clearly dominant because of the higher affinity of electrostatic binding sites (Bordbar et al., 1997).

It is noteworthy that the introduction of two or three Arg residues in close sequence proximity (cf. the double and triple mutants) decreases the sensitivity to C12-LAS. The sulfonate group should not be repelled by multiple positive charges, but a local concentration of charges with the same sign disfavors the binding of a ligand with hydrophobic groups, since these will decrease the dielectric constant of the local environment, and thus increase the repulsion among the charged groups.

The difference between GdmCl and C12-LAS is highlighted when we employ double-mutant cycles to analyze the interaction between individual residues. In this approach, two side chains are mutated singly and pairwise and the effect on $\Delta G_{N\text{-}U}$ or $\Delta G_{N\text{-}\ddagger}$ determined. The coupling energy between the two residues ΔG_{int} is defined as (Carter et al., 1984; Fersht et al., 1992):

$$\Delta G_{int} = \Delta\Delta G_{1.} + \Delta\Delta G_{1.+2.} - \Delta\Delta G_{1.+2.} \quad (4)$$

where $\Delta\Delta G_{1.}$, $\Delta\Delta G_{2.}$, and $\Delta\Delta G_{1.+2.}$ are the changes in the free energy of the two single and the double mutant, respectively. To yield readily interpretable data, the analysis requires that side chains are only truncated and no new groups are introduced. Nevertheless, if we subject the available double and triple mutants to such cycles (regarding the triple mutant A63R/N65R/D67R as a double mutant of A63R and N65R/D67R), we obtain a clear distinction between GdmCl and C12-LAS denaturation (Table 5). It is not surprising that the double mutant N65R/D67R is more destabilized than the sum of the individual mutations (leading to a negative value for ΔG_{int}), since two Arg residues in close proximity will repel each other. The further mutation of Ala63 to Arg (which in itself is destabilizing) leads to a positive value for ΔG_{int}, possibly because the structure relaxes and becomes more able to accommodate three positive charges in a small area. However, as far as C12-LAS is concerned, the presence of two or three Arg groups in close proximity leads to a synergistic stabilization ($\Delta G_{int} > 0$), because they prevent C12-LAS from binding for the reasons outlined above. This emphasizes once again the difference between solutes that interact strongly and those that interact weakly with the protein, namely that individual side-chain mutations can profoundly affect the mechanism of denaturation of the former, but not the latter.

Materials and methods

Preparation and purification of Cel45 mutants

For production of site-directed variants in fungal genes, the Chameleon double-stranded site-directed mutagenesis kit from Stratagene (La Jolla, California) was used. The mutated gene is positioned after the α-amylase promoter and in front of the transcription terminator and polyadenylation site from the *Aspergillus niger* glucoamylase (Christensen et al., 1988). The plasmid was transformed into the filamentous fungus *Aspergillus oryzae* strain A1560, which beforehand had been transformed with amdS using plasmid p3SR2 (Kelly & Hynes, 1985). This strain has been optimized by genetic manipulation to prevent it from producing its own amylase. The cellulase variants all contain a CBD and were purified by affinity chromatography, exploiting their binding to Avicel (cellulose swollen in phosphoric acid). Avicel in a slurry with buffer (20 mM sodium phosphate pH 7.5) was mixed with the production organism's extracellular fluid, in a ratio corresponding to 150 g Avicel per g total protein. After incubation at 4 °C for 20 min, the Avicel was packed into a 400 mL column. The column was washed with 200 mL buffer, followed by 0.5 M NaCl in buffer until no more protein eluted, and 500 mL 20 mM Tris pH 8.5. Finally, the pure full length enzyme was eluted with 1% triethylamine pH 11.8. All the cellulases were fully stable at this high pH. The eluted enzyme solution was adjusted to pH 8 and concentrated using an Amicon cell unit with a 20 kDa cut-off membrane (polypropylene DOW GR61PP) to 5 mg/L. The purified enzymes all gave a single band on SDS-PAGE.

Equilibrium denaturation fluorescence measurements

All experiments were carried out in 50 mM HEPES pH 7.0 at 25 °C. Typically, 10 μg/mL protein was incubated with 20–30 different concentrations of guanidinium chloride (GdmCl) for at least an hour at 25 °C before measuring the fluorescence on a thermostatted luminescence spectrophotometer (Perkin-Elmer, Foster City, California) using an excitation wavelength of 280 nm and an emission wavelength of 325 nm. The denaturation of the reduced protein was carried out as above with the addition of 10 mM DTT.

Equilibrium denaturation CD measurements

Far UV CD spectra (260–215 nm) were recorded on an Autodichrograph V (Jobin-Yvon, Longjumeau, France) in a 0.2 mm curvette at a concentra-tion of 2 mg/mL Cel45.

Table 5. *Interaction energies measured from double-mutant cycles*

1. mutation	2. mutation	Data	ΔG_{int} (kcal mol^{-1})[a]
D67R	N65R	Equilibrium denaturation	−1.21 ± 0.44
D67R	N65R	Kinetics of unfolding in GdmCl	0.41 ± 0.03
D67R	N65R	Kinetics of unfolding in C12-LAS	2.60
A63R	N65R/D67R	Equilibrium denaturation	0.87 ± 0.60
A63R	N65R/D67R	Kinetics of unfolding in GdmCl	0.09 ± 0.02
A63R	N65R/D67R	Kinetics of unfolding in C12-LAS	1.00

[a]Calculated according to Equation 4.

Analysis of equilibrium denaturation data

Data were analyzed according to a simple two-state unfolding model (Clarke & Fersht, 1993):

$$F = \frac{\alpha_U + \beta_U D + (\alpha_N + \beta_N D)10^{m_{N\text{-}U}(D\text{-}D^{50\%})}}{1 + 10^{m_{N\text{-}U}(D\text{-}D)^{50\%})}} \quad (5)$$

where F is the measured fluorescence, D is denaturant concentration, $m_{N\text{-}U}$ is the sensitivity of the log equilibrium constant of unfolding K to [GdmCl], $D^{50\%}$ is the [GdmCl] at which half the protein population is unfolded, α_U and α_N are the fluorescence levels of the unfolded and native states, and β_U and β_N are the sensitivities of α_U and α_N to denaturant concentration.

The free energy of destabilization for each mutant, $\Delta\Delta G_{N\text{-}U}$, is calculated as follows:

$$\Delta\Delta G_{N\text{-}U} = RT\ln(10) < m_{N\text{-}U} > (D^{50\%}_{wild\text{-}type} - D^{50\%}_{mutant}) \quad (6)$$

where $\langle m_{N\text{-}U}\rangle$ is the average value of $m_{N\text{-}U}$ for wild-type Cel45 and the 16 mutants ($4.94 \pm 0.28\ M^{-1}$).

Kinetics of denaturation using GdmCl

Unfolding was carried out by rapid 1:10 dilution of native protein into high concentrations of denaturant on an SX18-MV stopped-flow microanalyzer (Applied Photophysics, Leatherhead, UK) using an excitation wavelength of 280 nm and a 305 nm cut-off filter. Data were fitted to a double exponential equation. The slow phase typically amounted to 5–15% of the amplitude of the fast phase and 3–5% of the fast rate. The data from the slow phase were not used in the subsequent analysis. Refolding of Cel45 wild-type from the unfolded state (4 M GdmCl) was similarly measured by rapid 1:10 dilution into low concentrations of denaturant. Data were also fitted to a double exponential equation in which the two phases had similar amplitudes, although the slow rate constant only constituted 3–5% of the value of the fast rate constant.

Analysis of kinetic data

Unfolding data were analyzed by plotting $\log k_u$ vs. denaturant concentration and interpolating to 5 M GdmCl. The wild-type refolding and unfolding data were analyzed according to the following simple folding scheme:

$$U \overset{K_I}{\rightleftharpoons} I \underset{k_u}{\overset{k_f}{\rightleftharpoons}} N$$

where $K_I = [I]/[U]$ and k_f and k_u are rate constants. I and U are assumed to equilibrate within the deadtime of the stopped-flow mixing experiment (ca. 10 ms). This leads to the following equation:

$$\log k_{obs} = log\left(\frac{10^{\log k_f^{water} + m_f D}}{1 + 10^{-(\log K_I^{water} + m_I D)}} + 10^{\log k_u^{water} + a_u D + b_u D^2}\right) \quad (7)$$

where m_I and m_f are the linear dependencies of $\log K_I$ and $\log k_f$ on denaturant concentration; $\log k_u$ depends on D according to the parabolic relationship:

$$\log k_u = \log k_u^{water} + a_u D + b_u D^2 \quad (8)$$

where a_u and b_u are constants. We define m_u as

$$m_u = \partial \log(ku)/\partial[\text{GdmCl}] = a_u + 2 * b_u[D]. \quad (9)$$

The change in the activation energy of unfolding on mutation ($\Delta\Delta G_{N\text{-}\ddagger}$) at 5 M GdmCl is calculated as follows (Matouschek et al., 1989):

$$\Delta\Delta G^{5M}_{N\text{-}\ddagger} = RT\ln(10)\log\left(\frac{k_u^{wild\text{-}type,5\ M}}{k_u^{mutant,5\ M}}\right) \quad (10)$$

where R is the universal gas constant and T is the temperature (298 K). An analogous equation is used to calculate the destabilization in C12-LAS.

Kinetics of denaturation using C12-LAS

All solutions of C12-LAS (generously supplied by ECOSOL, Milano, Italy) were prepared from the powder and used the same day to avoid aging effects. Since unfolding of Cel45 in C12-LAS takes place over minutes rather than seconds, it was followed on an LS-50B Perkin-Elmer luminescence spectrophotometer by transferring concentrated protein solution to a thermostatted surfactant solution (in a 1:39 volume ratio) under rapid magnetic stirring, while monitoring fluorescence (excitation at 280 nm, emission at 345 nm).

Determination of C12-LAS' critical micelle concentration (CMC)

This was carried out using a Sigma 70 tensiometer (KSV Instruments, Helsinki, Finland) in 50 mM HEPES pH 7.0 at 25 °C. Small aliquots of a concentrated solution of C12-LAS were added incrementally to 100 mL buffer. The surface tension was measured after each addition. After plotting surface tension vs. log [C12-LAS], the CMC was estimated as the value of [C12-LAS] where the steep section of the graph (at low [C12-LAS]) intercepts the linear and almost flat section.

Acknowledgments

We thank ECOSOL for supplying the LAS detergents, Mikael Oliveberg for helpful discussions and critical comments, Margrethe Christensen for purifying mutants, and Kim V. Andersen for computer help. This work was funded in part by the European Union under contract BIO4-CT97-2303.

References

Arunachalam U, Kellis JT. 1996. Folding and stability of endoglucanase III: A single-domain cellulase from *Trichoderma reesei*. *Biochemistry 35*:11379–11385.

Baldwin RL. 1996. How Hofmeister ion interactions affect protein stability. *Biophys J 71*:2056–2063.

Bordbar AK, Saboury AA, Housaindokht MR, Moosavi-Movahedi AA. 1997. Statistical effects of the binding of ionic surfactant to protein. *J Colloid Interface Sci 192*:415–419.

Carter PJ, Winter G, Wilkinson AJ, Fersht AR. 1984. The use of double mutants to detect structural changes in the active site of the tyrosyl-tRNA synthetase (*Bacillus stearothermophilus*). *Cell 38*:835–840.

Casey JR, Reithmeier RAF. 1993. Detergent interaction with band 3, a model polytopic membrane protein. *Biochemistry 32*:1172–1179.

Choe SE, Matsudaira PT, Osterhout J, Wagner G, Shakhnovich EI. 1998. Folding kinetics of villin 14T: A protein domain with a central β-sheet and two hydrophobic cores. *Biochemistry 37*:14508–14518.

Christensen T, Wöldike H, Boel E, Mortensen SB, Hjortshøj K, Thim L, Hansen MT. 1988. High level expression of recombinant genes in *Aspergillus oryzae*. *Biotechnology 6*:1419–1422.

Clarke J, Fersht AR. 1993. Engineered disulfide bonds as probes of the folding pathway of barnase: Increasing the stability of proteins against the rate of denaturation. *Biochemistry 32*:4322–4329.

Clarke S. 1975. The size and detergent binding of membrane proteins. *J Biol Chem 250*:5459–5469.

Davies GJ, Dodson GG, Hubbard RE, Tolley SP, Dauter Z, Wilson KS, Hjort C, Mikkelsen JM, Rasmussen G, Schülein M. 1993. Structure and function of endoglucanase V. *Nature 365*:362–364.

Decker RV, Foster JF. 1966. The interaction of bovine plasma albumin with detergent anions. Stoichiometry and mechanism of binding of alkylbenzenesulfonates. *Biochemistry 5*:1242–1249.

Fersht AR, Itzhaki LS, ElMasry NF, Matthews JM, Otzen DE. 1994. Single versus parallel pathways of protein folding and fractional formation of structure in the transition state. *Proc Natl Acad Sci USA 91*:10426–10429.

Fersht AR, Matouschek A, Serrano L. 1992. The folding of an enzyme I: Theory of protein engineering analysis of stability and pathway of protein folding. *J Mol Biol 224*:771–782.

Hammond GS. 1955. A correlation of reaction rates. *J Am Chem Soc 77*:334–338.

Henrissat B, Bairoch A. 1993. New families in the classification of glycosyl hydrolases based on amino acid sequence similarities. *Biochem J 293*:781.

Ibel K, May RP, Kirschner K, Szadkowski H, Mascher E, Lundahl P. 1990. Protein-decorated micelle structure of sodium-dodecyl-sulfate-protein complexes as determined by neutron scattering. *Eur J Biochem 190*:311–318.

Ikai A. 1976. Stepwise degradation of serum low density lipoprotein by sodium dodecyl sulphate. *J Biochem 29*:679–688.

Jakobi G, Löhr A. 1987. *Detergents and textile washing—Principles and practice*. Weinheim, Berlin, Germany: VCH Publishers. Chapter 3.

Jeffries TW, Patel RN, Sykes MS, Klungness J. 1992. In: Rowell RM, Laufenberg TL, Rowell JK, eds. *Material interactions relevant to recycling of wood-based materials*. Pittsburgh, PA: Materials Research Society. pp 277–287.

Jirgensons B. 1967. Effects of n-propyl alcohol and detergents on the optical rotatory dispersion of α-chymotrypsinogen, β-casein, histone fraction 1 and soybean trypsin inhibitor. *J Biol Chem 242*:912–918.

Kelly JM, Hynes M. 1985. Transformation of *Aspergillus niger* by *amdS* gene of *Aspergillus nidulans*. *EMBO J 4*:475–479.

Kraulis PJ. 1991. MOLSCRIPT: A program to produce both detailed and schematic plots of protein structure. *J Appl Crystallogr 24*:946–950.

Kraulis PJ, Clore GM, Nilges M, Jones TA, Petterson G, Knowles J, Gronenborn AM. 1989. Determination of the three-dimensional solution structure of the C-terminal domain of cellobiohydrolase I from *Trichoderma reesei*. A study using nuclear magnetic resonance and hybrid distance geometry-dynamic simulated annealing. *Biochemistry 28*:7241–7257.

Lange NK. 1993. In: Suominen P, Reinikainen T, eds. *Trichoderma reesei cellulases and other hydrolases*. Helsinki: Foundation for Biotechnical and Industrial Fermentation. pp 263–272.

Makhatadze GI, Privalov PL. 1992. Protein interactions with urea and guanidinium chloride: A calorimetric study. *J Mol Biol 226*:491–505.

Makino S, Reynolds JA, Tanford C. 1973. The binding of deoxycholate and Triton-X 100 to protein. *J Biol Chem 248*:4926–4932.

Mascher E, Lundahl P. 1989. Sodium dodecyl sulphate-protein complexes. Changes in size and shape below the critical micelle concentration, as monitored by high-performance agarose gel chromatography. *J Chromatogr 476*:147–158.

Matouschek A, Fersht AR. 1993. Application of physical organic chemistry to engineered mutants of proteins—Hammond postulate behavior in the transition state of protein folding. *Proc Natl Acad Sci USA 90*:7814–7818.

Matouschek A, Kellis JT, Serrano L, Fersht AR. 1989. Mapping the transition state and pathway of protein folding by protein engineering. *Nature 340*:122–126.

Matouschek A, Otzen DE, Itzhaki LS, Jackson SE, Fersht AR. 1995. Movement of the position of the transition state in protein folding. *Biochemistry 34*:13656–13662.

Mattice WL, Riser JM, Clark DS. 1976. Conformational properties of the complexes formed by proteins and sodium dodecyl sulfate. *Biochemistry 15*:4264–4272.

Moriyama R, Makino S. 1985. Effect of detergent on protein structure. Action of detergents on secondary and oligomeric structures of band 3 from bovine erythrocyte membranes. *Biochim Biophys Acta 832*:135–141.

Nozaki Y, Tanford C. 1970. The solubility of amino acids, diglycine, and triglycine in aqueous guanidine hydrochloride solutions. *J Biol Chem 245*:1648–1652.

Otzen DE, Fersht AR. 1998. Folding of circular and permuted chymotrypsin inhibitor 2: Retention of the folding nucleus. *Biochemistry 37*:8139–8146.

Pace CN, Grimsley GR, Thomson JA, Barnett BJ. 1988. Conformational stability and activity of RNase T1 with zero, one and two intact disulfide bonds. *J Biol Chem 263*:11820–11825.

Parker MJ, Spencer J, Clarke AR. 1995. An integrated kinetic analysis of intermediates and transition states in protein folding reactions. *J Mol Biol 253*:771–786.

Rao P-F. 1989. Doctoral thesis. Faculty of Science, Osaka University.

Ray A, Raynolds J, Polet H, Steinhardt J. 1966. Binding of large organic anions and neutral molecules by native bovine serum albumin. *Biochemistry 5*:2606–2613.

Renthal R, Haas P. 1996. Effect of transmembrane helix packing on Trp and Tyr environments in detergent-solubilized bacterio-opsin. *J Protein Chem 15*:281–289.

Reynolds JA, Tanford C. 1970. The gross conformation of protein-sodium dodecyl sulfate complexes. *J Biol Chem 245*:5161–5165.

Serrano L, Matouschek A, Fersht AR. 1992. The folding of an enzyme III. Structure of the transition state for unfolding of barnase analyzed by a protein engineering procedure. *J Mol Biol 224*:805–818.

Tanford C. 1968. Protein denaturation. Part A. Characterization of the denatured state. *Adv Protein Chem 23*:121–217.

Tanford C. 1970. Protein denaturation. Part C. Theoretical models for the mechanism of denaturation. *Adv Prot Chem 24*:1–95.

Tanford C. 1991. *The hydrophobic effect. Formation of micelles and biological membranes*, 2nd ed. New York: Wiley & Sons.

Timasheff SN. 1993. The control of protein stability and association by weak interactions with water: How do solvents affect these processes? *Ann Rev Biophys Biomol Struct 22*:67–97.

Tomme P, Warren RAJ, Gilkes NR. 1995. Cellulose hydrolysis by bacteria and fungi. *Adv Microb Physiol 37*:1–81.

Turro NJ, Lei X-G, Ananthapadmanabhan KP, Aronson M. 1995. Spectroscopic probe analysis of protein-surfactant interactions: The BSA/SDS system. *Langmuir 11*:2525–2533.

Vanzi F, Madan B, Sharp K. 1998. Effects of the protein denaturants urea and guanidinium on water structure: A structural and thermodynamic study. *J Am Chem Soc 120*:10748–10753.

Yonath A, Podjarny A, Honig B, Sielecki A, Traub W. 1977. Crystallographic studies of protein denaturation and renaturation. 2. Sodium dodecyl sulfate induced structural changes in triclinic lysozyme. *Biochemistry 16*:1418–1424.